

"This is the peer reviewed version of the following article: [J. Am. Chem. Soc. 2020, 142, 5538–5542] which has been published in final form at [Link to final article using the DOI: <https://dx.doi.org/10.1021/jacs.0c01204>]. This article may be used for non-commercial purposes in accordance with the American Chemical Society Terms and Conditions for Self-Archiving."

Accessing the + IV Oxidation State in Molecular Complexes of Praseodymium.

Aurélien R. Willauer,^{a,‡} Chad T. Palumbo,^{a,‡} Farzaneh Fadaei-Tirani,^a Ivica Zivkovic,^b Iskander Douair,^c Laurent Maron,^c and Marinella Mazzanti^{a*}

^aInstitut des Sciences et Ingénierie Chimiques, Ecole Polytechnique Fédérale de Lausanne (EPFL), 1015, Lausanne, Switzerland

^bLaboratory for Quantum Magnetism, Institute of Physics, Ecole Polytechnique Fédérale de Lausanne (EPFL), 1015, Lausanne, Switzerland

^cLaboratoire de Physique et Chimie des Nano-objets, Institut National des Sciences Appliquées, 31077 Toulouse, Cedex 4, France

Supporting Information Placeholder

ABSTRACT: Out of the 14 lanthanide (Ln) ions, molecular complexes of Ln(IV) were known only for cerium and more recently terbium. Here we demonstrate that the +IV oxidation state is also accessible for the large praseodymium (Pr) cation. The oxidation of the tetrakis(triphenylsiloxide) Pr(III) ate complex, [KPr(OSiPh₃)₄(THF)₃], **1-Pr^{Ph}**, with [N(C₆H₄Br)₃][SbCl₆], affords the Pr(IV) complex [Pr(OSiPh₃)₄(MeCN)₂], **2-Pr^{Ph}**, which is stable once isolated. The solid state structure, UV-visible spectroscopy, magnetometry, and cyclic voltammetry data, along with the DFT computations of the **2-Pr^{Ph}** complex unambiguously confirm the presence of Pr(IV).

The most stable oxidation state for all lanthanide elements is the +3. However, in the last ten years, complexes of all lanthanides but one (Pm) have been synthesized in the + 2 oxidation state.¹ The high oxidizing power of Ce⁴⁺ has found important application in catalysis, rare earth separations, and materials science,² but, until 2019, cerium was the only lanthanide for

which the +4 oxidation state could be accessed in molecular complexes. In the last year, the first three examples of molecular complexes of Tb(IV) were reported by our group³ and others.⁴ In contrast, Pr(IV) has so far been observed only in extended oxide and fluoride materials.⁵ Previous attempts to prepare a Pr(IV) complex by oxidation of a Pr(III) precursor have so far only resulted in cation exchange⁶ or ligand oxidation.⁷

The calculated^{5a} Pr(IV)/Pr(III) reduction potential of + 3.4 V vs NHE is very close to the potential reported for the Tb(IV)/Tb(III) couple (+3.3 V vs NHE) suggesting that it may be possible to use similar supporting ligands and oxidizing condition to isolate molecular complexes of Pr(IV). Notably, electrochemical production of both Pr(IV) and Tb(IV) from concentrated carbonate solutions was reported more than forty years ago.⁸ However, preliminary attempts carried out in our group to synthesize a molecular Pr(IV) complex using the tris(tertbutoxy)siloxide ligand, which was

previously shown to stabilize homoleptic $[\text{Ln}(\text{OSi}(\text{O}^t\text{Bu})_3)_4]$ complexes of Ce(IV)⁹ and Tb(IV)^{3b}, did not allow the isolation of the Pr(IV) homologue probably due to the higher lability and higher coordination number of Pr which is one of the largest Ln ions.^{5a}

Here we show that the monodentate siloxide ligand $^-\text{OSiPh}_3$ allows the synthesis and characterization of the first example of a molecular complex of the 4f¹ Pr(IV) ion. The six-coordinate complex $[\text{Pr}^{\text{IV}}(\text{OSiPh}_3)_4(\text{MeCN})_2]$, **2-Pr^{Ph}**, was prepared by oxidation of the Pr(III) analogue, $[\text{KPr}(\text{OSiPh}_3)_4(\text{THF})_3]$, **1-Pr^{Ph}**, using $[\text{N}(\text{C}_6\text{H}_4\text{Br})_3][\text{SbCl}_6]$ as the oxidizing agent and was fully characterized by X-ray crystallography, cyclic voltammetry, magnetometry, and density functional theory calculations.

The potassium tetrakis(tertbutoxy)siloxide Pr(III) complex, $[\text{KPr}(\text{OSi}(\text{O}^t\text{Bu})_3)_4]$, **1-Pr^{O^tBu}**, was prepared in the same manner reported for Ce,^{9a} Gd,^{3b} and Tb,^{3b} from the reaction of $\text{KOSi}(\text{O}^t\text{Bu})_3$ with the anhydrous lanthanide trichloride in 70% yield. The molecular structure of **1-Pr^{O^tBu}** determined by X-ray crystallography shows that the Pr(III) complex is isostructural with the Ce(III) analogue $[\text{KCe}(\text{OSi}(\text{O}^t\text{Bu})_3)_4]$ (See supporting information).^{9a}

Tris(triphenylsiloxide)complexes of Ln(III) were already reported 30 years ago,¹⁰ but the Pr(III) potassium-tetrakis(triphenylsiloxide) $[\text{KPr}(\text{OSiPh}_3)_4(\text{THF})_3]$, **1-Pr^{Ph}** complex was not yet reported; we found its synthesis less straightforward than that of **1-Pr^{O^tBu}**. Reaction of the anhydrous trichloride praseodymium salt with 4 equiv. of KOSiPh_3 led to a mixture of **1-Pr^{Ph}** and the previously reported $[\text{Pr}(\text{OSiPh}_3)_3(\text{THF})_3]$ complex,¹¹ independent of the reaction temperature or time. However, addition of 1 equiv. KOSiPh_3 to the pure $[\text{Pr}(\text{OSiPh}_3)_3(\text{THF})_3]$ ¹¹ allowed the isolation of analytically pure **1-Pr^{Ph}** in 64% yield. The solid state structure of **1-Pr^{Ph}** (Figure 1) shows a 6-coordinate Pr(III) complex bound by four OSiPh_3 and two THF ligands in a distorted octahedral geometry. The structure of the six-coordinate **1-Pr^{Ph}** is similar to that reported for the five-coordinate Tb(III) complex in **1-Tb^{Ph}**^{3a} except that one additional THF ligand is bound to the Pr center. The OSiPh_3 ligands in **1-Pr^{Ph}** bind the potassium ion in close proximity to the Pr(III) ion. Addition of 2.2.2-cryptand to a THF-d₈ solution of **1-Pr^{Ph}** resulted in a shift, in the ¹H NMR spectrum, of the signals assigned to the ligand's

protons (Figure S7) suggesting that the potassium cation in **1-Pr^{Ph}** remains bound in solution.

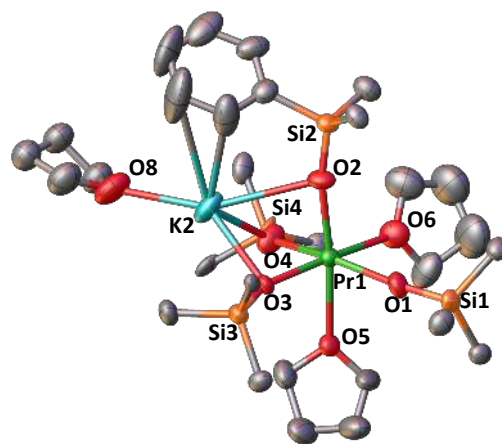


Figure 1. Solid-state molecular structure of **1-Pr^{Ph}** (50% probability ellipsoids). Hydrogens atoms, phenyl groups not bound to the potassium ion and the disordered K1 are omitted for clarity. Selected distances (Å): Pr1–O_{siloxide} range = 2.248(9) – 2.304(9); mean Pr1–O_{siloxide} = 2.27(2); Pr1–O_{THF} = 2.571(10) – 2.583(8).

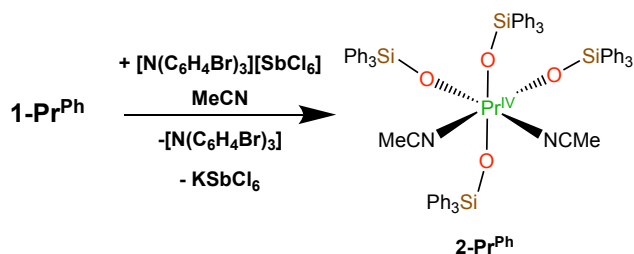
The addition of the strong oxidizing agent $[\text{N}(\text{C}_6\text{H}_4\text{Br})_3][\text{SbCl}_6]$,¹² to a MeCN solution of **1-Pr^{Ph}** or **1-Pr^{O^tBu}** resulted in the bleaching of the blue oxidant to yield orange/brown colored solutions. Any attempt to isolate the species formed in the oxidation of **1-Pr^{O^tBu}** resulted in the isolation of a Pr(III) decomposition product, showing the loss of a siloxide ligand and chloride coordination. The determined molecular structure of the decomposition product $[\{\text{Pr}^{\text{III}}(\text{OSi}(\text{O}^t\text{Bu})_3)_3\}_2(\mu\text{-Cl})_3(\mu\text{-K})_3]$, **3**, (see Supporting information) suggests that chloride binding to the praseodymium is likely to provide a decomposition pathway for the putative Pr(IV) intermediate species.

The isolation of the Pr(IV) complex $[\text{Pr}(\text{OSiPh}_3)_4(\text{MeCN})_2]$, **2-Pr^{Ph}**, formed by the oxidation reaction of **1-Pr^{Ph}**, turned out to be much more challenging compared to the isomorphous terbium complex $[\text{Tb}(\text{OSiPh}_3)_4(\text{MeCN})_2]$, **2-Tb^{Ph}**^{3a}. Notably, **2-Tb^{Ph}**^{3a} precipitates from solution as an orange solid immediately after addition of the oxidizing agent while **2-Pr^{Ph}** remains in solution and readily decomposes preventing isolation. We finally found that the isolation of **2-Pr^{Ph}** required a thorough drying under vacuum of the reaction mixture obtained immediately after addition of the oxidizing agent. Only after addition of fresh acetonitrile to the residue, **2-Pr^{Ph}** could be obtained as a brown solid in 55% yield (Scheme 1). The ¹H NMR spectrum of the isolated **2-Pr^{Ph}** complex

at 298 K in THF- d_8 shows one set of three signals at 7.8 ppm, 7.2 ppm, and 7.0 ppm for the 3 chemical shift inequivalent protons of the 12 phenyl groups, which is in agreement with the presence of a fluxional species (Figure S9). ^1H NMR studies in THF- d_8 showed that **2-Pr^{Ph}** is more stable in solution once isolated and separated from the oxidation byproducts; approximately 70% of **2-Pr^{Ph}** is still observed in the ^1H NMR spectrum after 3 hours at room temperature (Figure S11) whereas in the reaction mixture, freshly generated **2-Pr^{Ph}** decomposes completely within 3 hours (Figure S12). In both decomposition experiments, $[\text{Pr}(\text{OSiPh}_3)_3(\text{THF})_3]$ was produced as the only identifiable product (Figure S11 and S12).

The UV-Visible spectrum of **2-Pr^{Ph}** measured immediately after dissolution in THF showed a broad absorption maximum located at a lower energy $\lambda_{\text{max}} = 363 \text{ nm}$ ($\epsilon = 3800 \text{ M}^{-1} \text{ cm}^{-1}$) (Figure S14) compared to that reported for solutions of Pr(IV) species electrochemically generated in aqueous carbonate medium ($\lambda_{\text{max}} = 283 \text{ nm}$, $\epsilon > 1000 \text{ M}^{-1} \text{ cm}^{-1}$)⁸.

Crystals of **2-Pr^{Ph}** suitable for characterization by X-ray diffraction were obtained upon storage of a saturated MeCN solution of **2-Pr^{Ph}** at $-40 \text{ }^\circ\text{C}$ overnight.



Scheme 1. Synthesis of $[\text{Pr}(\text{OSiPh}_3)_4(\text{MeCN})_2]$, **2-Pr^{Ph}**.

The complex **2-Pr^{Ph}** crystallizes in the orthorhombic space group $Pca2_1$ and is isomorphous with the previously reported Tb(IV) complex $[\text{Tb}(\text{OSiPh}_3)_4(\text{MeCN})_2]$, **2-Tb^{Ph}**.^{3a} The molecular structure of **2-Pr^{Ph}** shows a six-coordinate Pr(IV) ion bound by four κ^1 triphenylsiloxide ligands and two molecules of acetonitrile in a distorted octahedral coordination geometry (Figure 2). The differences in the Ln-O_{siloxide} bond distances (see Table S5) between **2-Pr^{Ph}** and **2-Tb^{Ph}** are smaller than the 0.09 Å difference expected on the basis of their 6-coordinate Shannon ionic radii (Pr(IV), 0.85 Å, Tb(IV), 0.76 Å).¹³ The smaller than expected changes could be indicative of increased covalency in Ln(IV) complexes.¹⁴

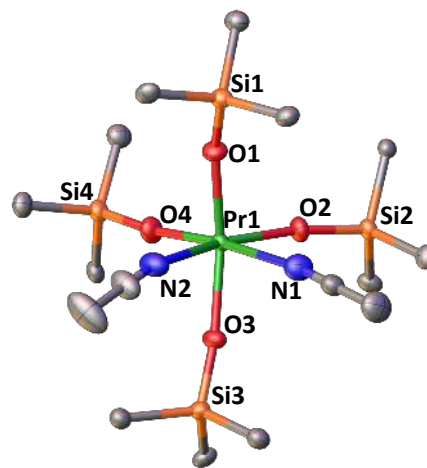


Figure 2. Solid-state molecular structure of **2-Pr^{Ph}** (50 % probability ellipsoids). Hydrogens atoms, phenyl groups, residual solvent molecules and a second molecule of **2-Pr^{Ph}** present in the unit cell are omitted for clarity. Selected distances (Å): Pr1-O_{siloxide} range = 2.088(4) – 2.121(4); mean Pr1-O_{siloxide} = 2.10(1); Pr1-N = 2.599(6) – 2.603(6).

The X-band EPR spectra of the **1-Ce^{Ph}** (4f¹), **2-Pr^{Ph}** (4f¹), and **1-Pr^{Ph}** (4f²) complexes measured at 5 K as frozen toluene or THF solutions did not show any signal. The absence of EPR signal for f¹ species has been observed in several examples of 5f¹ U(V) complexes.¹⁵

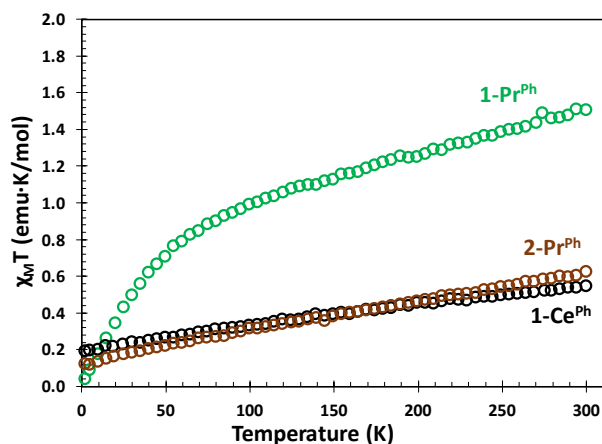


Figure 3. Plot of $\chi_{\text{M}}T$ versus temperature data for ground solid samples of **1-Pr^{Ph}** (green), **2-Pr^{Ph}** (brown), and **1-Ce^{Ph}** (black) collected under an applied magnetic field of 1 T.

The $\chi_{\text{M}}T$ versus T data (χ_{M} = molar magnetic susceptibility) measured for **2-Pr^{Ph}** overlap with those measured for **1-Ce^{Ph}** in the temperature range 300 to 2 K as anticipated for an isoelectronic 4f¹ ion, Figure 3. In contrast, the $\chi_{\text{M}}T$ versus T and χ_{M} versus T data of **1-Pr^{Ph}** are typical of an f² ion. The $\chi_{\text{M}}T = 0.622$ and 0.544 emu·K/mol measured at 300 K for **2-Pr^{Ph}** and **1-Ce^{Ph}**,

respectively, are in agreement with the $\chi_M T = 0.8$ emu·K/mol predicted for a $4f^1$ complex and much lower than the 1.5 emu·K/mol found for the $4f^2$ Pr(III) in **1-Pr^{Ph}** (predicted 1.6 emu·K/mol).

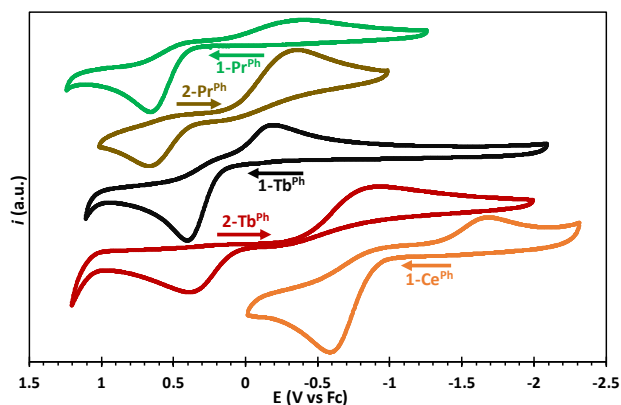


Figure 4. Cyclic voltammograms of 2 mM solutions of **1-Pr^{Ph}** (green), **2-Pr^{Ph}** (brown), **1-Tb^{Ph}** (black)^{3a}, **2-Tb^{Ph}** (red),^{3a} and **1-Ce^{Ph}** (orange) measured in 0.1 M [NBu₄][B(C₆F₅)] in THF versus vs Fc/Fc⁺ with a glassy carbon working electrode. The measurements were performed at room temperature and scanned at 100 mV/s.

Cyclic voltammetry experiments were performed in THF as 2 mM solutions of the tetrakis(triphenylsiloxide) praseodymium complexes **1-Pr^{Ph}** and **2-Pr^{Ph}**. The measurements were performed with 0.1 M [NBu₄][B(C₆F₅)] as the supporting electrolyte (Figure 4, Table S4). The cyclic voltammogram of **2-Pr^{Ph}** shows a metal-based reduction feature at $E_{pc} = -0.38$ V vs Fc/Fc⁺ and a related oxidation feature at $E_{pa} = 0.67$ V vs vs Fc/Fc⁺ with a peak separation of $\Delta E = 1.05$ V (at a scan rate of 100 mV/s). This oxidation event is occurring at a potential 0.18 V more positive than that of the Tb(IV) analogue **2-Tb^{Ph}** ($E_{pc} = 0.49$ V vs Fc/Fc⁺ at a scan rate of 100 mV/s)^{3a} and is in agreement with the difference between their respective calculated redox potentials.^{5a} However, the reduction wave of **2-Pr^{Ph}** is identified at a potential 0.58 V more positive than for **2-Tb^{Ph}** ($E_{pa} = -0.96$ V vs Fc/Fc⁺ at a scan rate of 100 mV/s). This suggests an easier reduction of the +IV to the +III oxidation state for the praseodymium than for terbium complexes and therefore a lower kinetic stability of the Pr(IV) species.

DFT (B3PW91) calculations were carried out on compounds **1-Pr^{Ph}** and **2-Pr^{Ph}** in order to further confirm the +IV oxidation state of Pr in **2-Pr^{Ph}**. The optimized geometries of **1-Pr^{Ph}** and **2-Pr^{Ph}** compare well with their experimental structures (see Supporting Information). Among other things, the Pr–O bond

distances are well reproduced (2.09–2.12 Å vs. 2.08–2.12 Å experimentally for **2-Pr^{Ph}**) and are significantly shorter than in **1-Pr^{Ph}** (2.25–2.30 Å vs. 2.24–2.30 experimentally). This shortening is in line with the oxidation of the Pr center from +III in **1-Pr^{Ph}** to +IV in **2-Pr^{Ph}**. A similar situation was observed for the oxidation of Tb(III) to Tb(IV), pointing in the direction of the +IV oxidation state in **2-Pr^{Ph}**. To further gain confidence on this assignment, the unpaired spin density of the two compounds was computed and plotted (Figure 5). First of all, the unpaired spin density is in both cases only located at the Pr center, ruling out the possibility of Pr(III)-ligand radical **2-Pr^{Ph}**. An unpaired spin density of 1.1 is found for **2-Pr^{Ph}**, in line with a Pr(IV), whereas it is 2.03 in **1-Pr^{Ph}** as expected for a Pr(III) complex. NBO analysis indicates that the Pr–O Wiberg Bond Indexes (WBI) are 0.85 higher than for the Tb(IV) analog (0.60–0.65) indicating a more covalent interaction in Pr(IV) than in Tb(IV). In **2-Pr^{Ph}**, NBO shows very strong donations from the oxygen lone pairs (sp) to empty s/d/f hybrid orbitals on Pr (donation of more than 130 kcal/mol at the second-order donor-acceptor level indicative of bond presence).

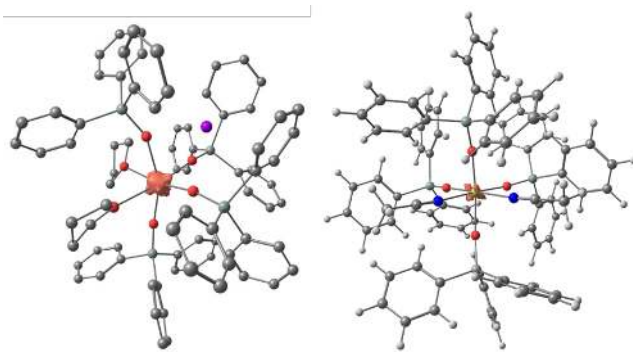


Figure 5. Spin density plot of **1-Pr^{Ph}** (left) and **2-Pr^{Ph}** (right) showing that the unpaired electrons are only located on the metal and only arising from f orbitals.

In conclusion, we showed that, despite its higher kinetic lability, it is possible to stabilize the Pr(IV) cation as an isolable molecular complex by using electron-rich triphenylsiloxide ligands and carefully chosen reaction conditions. The presence of Pr(IV) was unambiguously identified by X-ray crystallography, magnetometry, cyclic voltammetry, and our results were corroborated with density functional theory calculations. The Pr(IV) tetrasiloxide complex is isomorphous with its Tb(IV) analogue but DFT studies indicate greater

covalency with respect to the Ln–O interaction in **2-Pr^{Ph}**. These results extend the +4 oxidation state to molecular complexes of Pr(IV) providing important opportunities to study bonding, and expand the redox reactivity and separations chemistry of lanthanides.

ASSOCIATED CONTENT

Supporting Information

The Supporting Information is available free of charge on the ACS Publications website at DOI: 1021/XXX and includes additional spectroscopic, electrochemical characterization, magnetism, and structural details for **1-Pr^{OtBu}**, **1-Ln^{Ph}** (Ln = Ce, Pr), **2-Pr^{Ph}**, and **3** (PDF). Crystallographic data in CIF format for **1-Pr^{OtBu}**, **1-Pr^{Ph}**, **2-Pr^{Ph}**, and **3** (CIF).

AUTHOR INFORMATION

Corresponding Author

*marinella.mazzanti@epfl.ch

Orcid Number

Aurélien R. Willauer: 0000-0002-0699-6895

Chad T. Palumbo: 0000-0001-6436-4602

Farzaneh Fadaei-Tirani: 0000-0001-8161-8715

Ivica Zivkovic: 0000-0003-0366-8199

Laurent Maron: 0000-0003-2653-8557

Marinella Mazzanti: 0000-0002-3427-008X

Author Contributions

‡These authors contributed equally.

Notes

The authors declare no competing financial interests.

ACKNOWLEDGMENT

We acknowledge support from the Swiss National Science Foundation grant number 178793 and the Ecole Polytechnique Fédérale de Lausanne (EPFL). We thank Dr. R. Scopelliti for important contributions to the X-ray single crystal structure analyses.

REFERENCES

1. (a) Fieser, M. E.; MacDonald, M. R.; Krull, B. T.; Bates, J. E.; Ziller, J. W.; Furche, F.; Evans, W. J., Structural, Spectroscopic, and Theoretical Comparison of Traditional vs Recently Discovered Ln(2+) Ions in the K(2.2.2-cryptand)(C₅H₄SiMe₃)(3)Ln Complexes: The Variable Nature of Dy²⁺ and Nd²⁺. *J. Am. Chem. Soc.* **2015**, *137*, 369-382; (b) Hitchcock, P. B.; Lappert, M. F.; Maron, L.; Protchenko, A. V., Lanthanum does form stable molecular compounds in the +2 oxidation state. *Angew. Chem. Int. Ed. Engl.* **2008**, *47*, 1488-1491; (c) MacDonald, M. R.; Bates, J. E.; Ziller, J. W.; Furche, F.; Evans, W. J., Completing the Series of +2 Ions for the Lanthanide Elements: Synthesis of Molecular Complexes of Pr²⁺, Gd²⁺, Tb²⁺, and Lu²⁺. *J. Am. Chem. Soc.* **2013**, *135*, 9857-9868; (d) MacDonald, M. R.; Bates, J. E.; Fieser, M. E.; Ziller, J. W.; Furche, F.; Evans, W. J., Expanding Rare-

Earth Oxidation State Chemistry to Molecular Complexes of Holmium(II) and Erbium(II). *J. Am. Chem. Soc.* **2012**, *134*, 8420-8423. 2. (a) Anwander, R.; Dolg, M.; Edlmann, F. T., The difficult search for organocerium(IV) compounds. *Chem. Soc. Rev.* **2017**, *46*, 6697-6709; (b) Kaltsoyannis, N.; Scott, P., *The f elements*. Oxford University Press: Oxford, 1999; (c) So, Y. M.; Leung, W. H., Recent advances in the coordination chemistry of cerium(IV) complexes. *Coord. Chem. Rev.* **2017**, *340*, 172-197; (d) Drose, P.; Crozier, A. R.; Lashkari, S.; Gottfriedsen, J.; Blaurock, S.; Hrib, C. G.; Maichle-Mossmer, C.; Schadle, C.; Anwander, R.; Edlmann, F. T., Facile Access to Tetravalent Cerium Compounds: One-Electron Oxidation Using Iodine(III) Reagents. *J. Am. Chem. Soc.* **2010**, *132*, 14046-14047; (e) Klamm, B. E.; Windorff, C. J.; Marsh, M. L.; Meeker, D. S.; Albrecht-Schmitt, T. E., Schiff-base coordination complexes with plutonium(IV) and cerium(IV). *Chem. Commun.* **2018**, *54*, 8634-8636; (f) Schelter, E. J., Cerium under the lens. *Nat. Chem.* **2013**, *5*, 348-348; (g) Montini, T.; Melchionna, M.; Monai, M.; Fornasiero, P., Fundamentals and Catalytic Applications of CeO₂-Based Materials. *Chem. Rev.* **2016**, *116*, 5987-6041; (h) Sridharan, V.; Menendez, J. C., Cerium(IV) Ammonium Nitrate as a Catalyst in Organic Synthesis. *Chem. Rev.* **2010**, *110*, 3805-3849; (i) Pham, T. A.; Altman, A. B.; Stieber, S. C. E.; Booth, C. H.; Kozimor, S. A.; Lukens, W. W.; Olive, D. T.; Tylliszczak, T.; Wang, J.; Minasian, S. G.; Raymond, K. N., A Macrocyclic Chelator That Selectively Binds Ln(4+) over Ln(3+) by a Factor of 10(29). *Inorg. Chem.* **2016**, *55*, 9989-10002; (j) Broderick, E. M.; Diaconescu, P. L., Cerium(IV) Catalysts for the Ring-Opening Polymerization of Lactide. *Inorg. Chem.* **2009**, *48*, 4701-4706; (k) Piro, N. A.; Robinson, J. R.; Walsh, P. J.; Schelter, E. J., The electrochemical behavior of cerium(III/IV) complexes: Thermodynamics, kinetics and applications in synthesis. *Coord. Chem. Rev.* **2014**, *260*, 21-36; (l) Damon, P. L.; Wu, G.; Kaltsoyannis, N.; Hayton, T. W., Formation of a Ce(IV) Oxo Complex via Inner Sphere Nitrate Reduction. *J. Am. Chem. Soc.* **2016**, *138*, 12743-12746; (m) Qiao, Y. S.; Schelter, E. J., Lanthanide Photocatalysis. *Acc. Chem. Res.* **2018**, *51*, 2926-2936; (n) Sroor, F. M. A.; Edlmann, F. T., Lanthanides: Tetravalent Organometallic. In *Encycl. Inorg. Bioinorg. Chem.*, Scott, R. A., Ed.; John Wiley & Sons: Hoboken, NJ, **2012**; 1-14; (o) Cheisson, T.; Schelter, E. J., Rare earth elements: Mendeleev's bane, modern marvels. *Science* **2019**, *363*, 489-493. 3. (a) Willauer, A.; Palumbo, C. T.; Scopelliti, R.; Zivkovic, I.; Douair, I.; Laurent, S.; Mazzanti, M., Stabilization of the Oxidation State +IV in Siloxide-Supported Terbium Compounds. *Angew. Chem. Int. Ed. Engl.* **2020**, *59*, 3549-3553.; (b) Palumbo, C. T.; Zivkovic, I.; Scopelliti, R.; Mazzanti, M., Molecular Complex of Tb in the +4 Oxidation State. *J. Am. Chem. Soc.* **2019**, *141*, 9827-9831. 4. Rice, N. T.; Popov, I. A.; Russo, D. R.; Bacsa, J.; Batista, E. R.; Yang, P.; Telsler, J.; La Pierre, H. S., Design, Isolation, and Spectroscopic Analysis of a Tetravalent Terbium Complex. *J. Am. Chem. Soc.* **2019**, *141*, 13222-13233. 5. (a) Cotton, S., *Lanthanides and Actinides Chemistry*. John Wiley & Sons: Chichester, 2006; (b) Tezuka, K.; Hinatsu, Y., Electron paramagnetic resonance study of Pr⁴⁺ ions doped in BaHfO₃ perovskite. *J. Solid State Chem.* **2001**, *156*, 203-206; (c) Fiscus, J. E.; zur Loye, H. C., Synthesis of Sr₂PrO₄: a Pr⁴⁺-containing oxide in the Sr₂PbO₄ structure type. *J. Alloys Compd.* **2000**, *306*, 141-145; (d) Hinatsu, Y.; Itoh, M.; Edelstein, N., Structure and magnetic properties of tetravalent praseodymium perovskite SrPrO₃. *J. Solid State Chem.* **1997**, *132*, 337-341; (e) Hinatsu, Y., Magnetic-susceptibility and electron-paramagnetic resonance-spectrum of tetravalent praseodymium ions in BaPrO₃. *J. Solid State Chem.* **1993**, *102*, 362-367. 6. Gregson, M.; Lu, E.; Mills, D. P.; Tuna, F.; McInnes, E. J. L.; Hennig, C.; Scheinost, A. C.; McMaster, J.; Lewis, W.; Blake, A. J.; Kerridge, A.; Liddle, S. T., The inverse-trans-influence in tetravalent lanthanide and actinide bis(carbene) complexes. *Nat. Commun.* **2017**, *8*, 14137. 7. (a) Kim, J. E.; Bogart, J. A.; Carroll, P. J.; Schelter, E. J., Rare Earth Metal Complexes of Bidentate Nitroxide Ligands: Synthesis and Electrochemistry. *Inorg. Chem.* **2016**, *55*, 775-784; (b)

- Noh, W.; Girolami, G. S., X-ray crystal structure of the tetra(tert-butyl)erbate anion and attempts to prepare tetravalent organolanthanide complexes. *Polyhedron* **2007**, *26*, 3865-3870.
8. Hobart, D. E.; Samhoun, K.; Young, J. P.; Norvell, V. E.; Mamantov, G.; Peterson, J. R., Stabilization of praseodymium(IV) and terbium(IV) in aqueous carbonate solution. *Inorg. Nucl. Chem. Letters* **1980**, *16*, 321-328.
9. (a) Kelly, R. P.; Maron, L.; Scopelliti, R.; Mazzanti, M., Reduction of a Cerium(III) Siloxide Complex To Afford a Quadruple-Decker Arene-Bridged Cerium(II) Sandwich. *Angew. Chem. Int. Ed. Engl.* **2017**, *56*, 15663-15666; (b) Friedrich, J.; Qiao, Y. S.; Maichle-Mossmer, C.; Schelter, E. J.; Anwender, R., Redox-enhanced hemilability of a tris(tert-butoxy) siloxy ligand at cerium. *J. Chem. Soc.-Dalton Trans.* **2018**, *47*, 10113-10123; (c) Friedrich, J.; Maichle-Mossmer, C.; Anwender, R., Synthesis and derivatisation of ceric tris(tert-butoxy)siloxides. *Chem. Commun.* **2017**, *53*, 12044-12047.
10. (a) Evans, W. J.; Golden, R. E.; Ziller, J. W., A comparative synthetic and structural study of triphenylmethoxide and triphenylsiloxide complexes of the early lanthanides, including x-ray crystal-structures of $\text{La}_2(\text{OCPh}_3)_6$ and $\text{Ce}_2(\text{OSiPh}_3)_6$. *Inorg. Chem.* **1991**, *30*, 4963-4968; (b) McGearry, M. J.; Coan, P. S.; Foltz, K.; Streib, W. E.; Caulton, K. G., Yttrium and lanthanum silyloxy complexes. *Inorg. Chem.* **1991**, *30*, 1723-1735.
11. Gradeff, P. S.; Yunlu, K.; Deming, T. J.; Olofson, J. M.; Doedens, R. J.; Evans, W. J., Synthesis of yttrium and lanthanide silyloxy complexes from anhydrous nitrate and oxo alkoxide precursors and the X-ray crystal-structure of $\text{Ce}(\text{OSiPh}_3)_3(\text{THF})_3$ (THF). *Inorg. Chem.* **1990**, *29*, 420-424.
12. Connelly, N. G.; Geiger, W. E., Chemical redox agents for organometallic chemistry. *Chem. Rev.* **1996**, *96*, 877-910.
13. Shannon, R. D., Revised Effective Ionic-Radii and Systematic Studies of Interatomic Distances in Halides and Chalcogenides. *Acta Crystallogr A* **1976**, *32*, 751-767.
14. Minasian, S. G.; Batista, E. R.; Booth, C. H.; Clark, D. L.; Keith, J. M.; Kozimor, S. A.; Lukens, W. W.; Martin, R. L.; Shuh, D. K.; Stieber, S. C. E.; Tyliczcak, T.; Wen, X. D., Quantitative Evidence for Lanthanide-Oxygen Orbital Mixing in CeO_2 , PrO_2 , and TbO_2 . *J. Am. Chem. Soc.* **2017**, *139*, 18052-18064.
15. (a) Rosen, R. K.; Andersen, R. A.; Edelstein, N. M., $(\text{MeC}_5\text{H}_4)_2\text{U}_2\text{Mu}-1,4\text{-N}_2\text{C}_6\text{H}_4$ - a Bimetallic Molecule with Antiferromagnetic Coupling between the Uranium Centers. *J. Am. Chem. Soc.* **1990**, *112*, 4588-4590; (b) Castro-Rodriguez, I.; Olsen, K.; Gantzel, P.; Meyer, K., Uranium tris-aryloxy derivatives supported by triazacyclononane: Engendering a reactive uranium(III) center with a single pocket for reactivity. *J. Am. Chem. Soc.* **2003**, *125*, 4565-4571; (c) Nocton, G.; Horeglad, P.; Vetere, V.; Pécaut, J.; Dubois, L.; Maldivi, P.; Edelstein, N. M.; Mazzanti, M., Synthesis, Structure, and Bonding of Stable Complexes of Pentavalent Uranyl. *J. Am. Chem. Soc.* **2010**, *132*, 495-508.

